Cross-Domain Consistent Fingerprint Denoising

Indu Joshi, Tashvik Dhamija, Rohit Kumar, Antitza Dantcheva, Sumantra Dutta Roy, Prem Kumar Kalra

Sensors Letters

Cross-Domain Consistent Fingerprint Denoising

Indu Joshi[1,2], Tashvik Dhamija[3], Rohit Kumar[3], Antitza Dantcheva[1], Sumantra Dutta Roy[2] and Prem Kumar Kalra[2]

[1]Inria Sophia Antipolis, France [2]IIT Delhi, India [3]Delhi Technological University, India

Abstract—Performance of state-of-the-art fingerprint denoising model on poor quality fingerprints degrades due to *cross-domain shift* observed between training and testing domains. To address this limitation, we present a *cross-domain consistent* fingerprint denoising model, which ensures that the output of two fingerprint images with the same ridge structure, however varying contrast and ridge-valley clarity should be similar. Results indicate that the proposed CDC-GAN outperforms state-of-the-art fingerprint denoising algorithms on challenging publicly available poor quality fingerprint databases.

Index Terms—Fingerprints, Denoising, Biometrics.

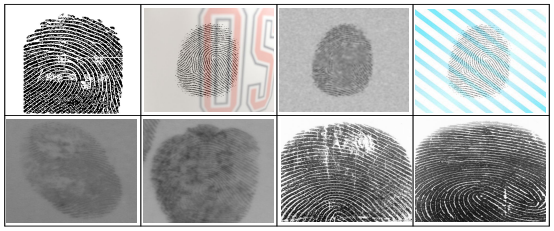

Fig. 1. A fingerprint denoising model is trained on synthetically distorted fingerprints (first row) and tested on real poor quality fingerprints (last row). *Cross-domain shift* observed between the training and testing data leads to unsatisfactory fingerprint denoising performance.

I. INTRODUCTION AND RELATED WORK

Automated fingerprint recognition systems are widely used for access control, and law enforcement applications [1]–[7]. The fingerprint denoising module is a key part of a fingerprint recognition system. A fingerprint denoising algorithm improves the clarity of ridges and valleys, removes structured background noise, and predicts missing ridge information in poor quality fingerprint regions. As a result, effective fingerprint denoising helps to correctly extract ridge features, including minutiae, and obtain improved fingerprint matching performance. However, due to the lack of annotations for training a fingerprint denoising model, the model is trained on synthetically distorted fingerprints and later tested on real poor quality fingerprints (see Figure 1). However, the *cross-domain shift* observed between training (source), and testing (target) domains leads to poor generalization on challenging real poor quality fingerprints. To address this limitation of state-of-the-art fingerprint denoising models, this paper introduces *Cross-Domain Consistent Generative Adversarial Network* (CDC-GAN), which exploits an unsupervised consistency regularization loss in both source and target domains to ensure cross-domain consistency in predictions of a fingerprint denoising model.

Classical methods for fingerprint denoising exploit contextual information [8] such as ridge orientations [9] to approximate the ridge structure in poor quality fingerprint regions. Filtering both in spatial [10] and frequency domain [11] are widely used classical methods for fingerprint denoising. Recent deep learning based fingerprint denoising models translate a poor quality fingerprint into a better quality one using an encoder-decoder backbone [12]–[19]. A detailed survey on fingerprint denoising methods is presented in [20]. We note that due to lack of annotated training dataset, all these methods [12], [14]–[19] are trained on synthetically distorted fingerprints. Subsequently, these methods are adversarially affected by the *cross-domain shift* observed between the training (source) and the testing (target) domains.

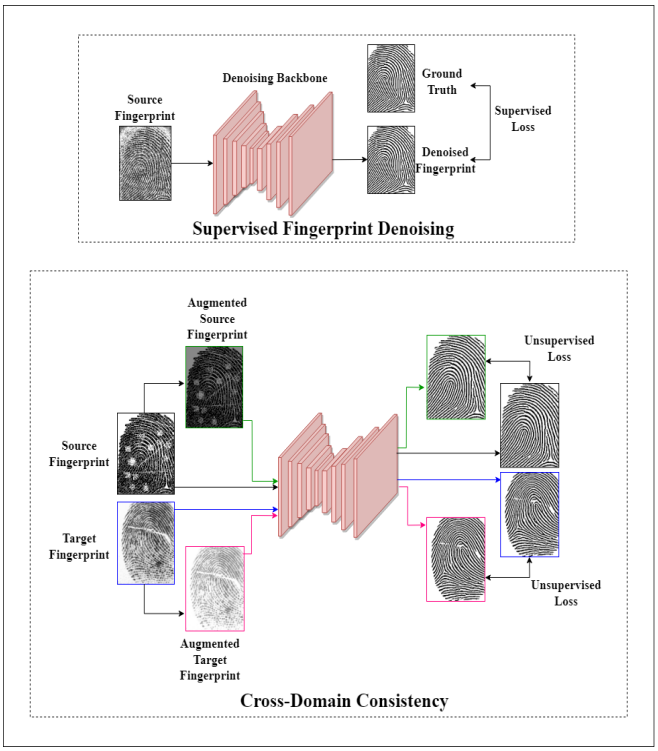

Fig. 2. Flowchart illustrating that the proposed CDC-GAN exploits *supervised loss* ($\mathcal{L}_{den}$) by training on synthetically distorted and corresponding good quality binarized fingerprints (source domain). Additionally, to enforce cross-domain consistency, an *unsupervised loss* ($\mathcal{L}_{cdc}$) is introduced to ensure output for augmented and original fingerprint samples (of both source and target domain) are similar.

Research Contributions: To address the cross-domain shift, we propose a novel *Cross-Domain Consistent Generative Adversarial Network* (CDC-GAN) that is trained to ensure *cross-domain consis-*

Corresponding author: I. Joshi (e-mail: indu.joshi@inria.fr).

tency. To the best of our knowledge, this is the *first work* to introduce a consistency regularization technique in the fingerprint denoising domain. The cross-domain consistency regularization ensures that the fingerprints with the same ridge structure, however, varying backgrounds and contrast have similar outputs. Additionally, an ablation study is conducted to provide insights on the individual contribution of introducing consistency in source and target domains. Results on challenging publicly available rural Indian fingerprints and latent fingerprints signify superior denoising ability of the proposed CDC-GAN compared to state-of-the-art.

II. PROPOSED METHOD

The proposed CDC-GAN is a deep neural network that is trained to translate a poor quality grayscale fingerprint image to a binarized fingerprint image with enhanced ridge-valley clarity. In order to mitigate the cross-domain gap observed between training (source) and testing (target) domains, in addition to a supervised fingerprint denoising loss in the source domain, the proposed CDC-GAN introduces an unsupervised cross-domain consistency loss in both source and target domains. The schematic diagram of CDC-GAN is presented in Figure 2. To formalize, let X_s signifies the distribution of distorted fingerprints in the source domain and corresponding labelled denoised fingerprints. X_t signifies the distributions of unlabelled fingerprints in the target domain. $X_s = \{(x_s, y_s)\}$ and $X_t = \{x_t\}$. L_{den} signifies the baseline fingerprint denoising loss. $o(x_s)$ signifies the denoised fingerprint generated by the proposed CDC-GAN. $X_{ul} = \{(x'_s \in X_s) \cup (x_t \in X_t)\}$. We note that x'_s signifies an unlabelled fingerprint sample from the source domain.

$$\mathcal{L}_{den}(X_s) = \sum_{(x_s, y_s) \in X_s} L_{den}(o(x_s), y_s) \tag{1}$$

$$\mathcal{L}_{cdc}(X_{ul}) = \sum_{x_{ul} \in X_{ul}} ||o(x_{ul}) - o(T(x_{ul}))||_1 \tag{2}$$

$$\mathcal{L}_{total} = \mathcal{L}_{den}(X_s) + \alpha \mathcal{L}_{cdc}(X_{ul}) \tag{3}$$

$\mathcal{L}_{cdc}$ is an unsupervised loss that ensures consistency among the output of the CDC-GAN such that the output for the input sample x_{ul} is similar to the output of the augmented sample $T(x_{ul})$. Baseline fingerprint denoising loss L_{den} and model architecture are adopted from [16]. The value of α is empirically chosen to be 1 and 0.01 for the rural and latent fingerprints respectively. For the rural Indian fingerprint database, changing the contrast and brightness while for latent fingerprints, Gaussian blurring empirically turns out to be the most effective augmentation. The choice of these augmentations seems intuitive as the poor ridge-valley clarity observed in poor quality rural Indian fingerprints and smudged patterns observed in latent fingerprints are well represented by changing in contrast and Gaussian blurring, respectively.

Implementation Details: The proposed CDC-GAN is a ResNet based generative adversarial network [16] with an encoder-decoder based network architecture with a total of 14141634 trainable parameters. The model is implemented from scratch in Python using the PyTorch library, version v1.11.0. The network is trained using an Adam optimizer with a learning rate of 0.0002. The model is trained with a batch size of 2 images. The training is conducted on a GPU node with four NVIDIA GTX 1080 Ti GPU cards with 11GB RAM per card and an E5-2620v4 CPU with 128GB RAM per node.

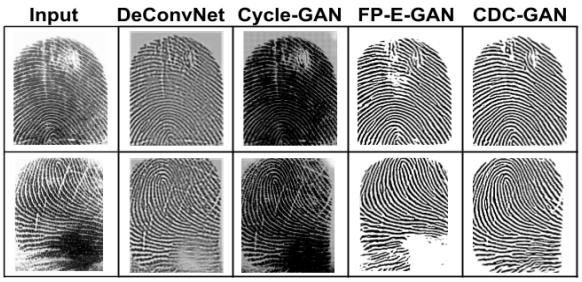

Fig. 3. Sample rural Indian fingerprints [21] demonstrating the superior fingerprint denoising ability of the proposed CDC-GAN compared to state-of-the-art.

TABLE 1. Average NFIQ fingerprint quality scores achieved on the Rural Indian fingerprint database [21].

Denoising Algorithm	NFIQ Score (↓)
Raw Image	2.94
Hong *et al.* [10]	2.05
DeconvNet [12]	1.95
Cycle-GAN [14]	1.76
FP-E-GAN [16]	1.31
CDC-GAN	**1.30**

TABLE 2. Average equal error rate (EER) obtained on the Rural Indian fingerprint database [21].

Denoising Algorithm	Bozorth (↓)	MCC (↓)
Raw Image	16.36	13.23
Hong *et al.* [10]	11.01	11.46
DeConvNet [12]	10.93	10.86
Cycle-GAN [14]	29.52	27.96
FP-E-GAN [16]	7.30	5.96
CDC-GAN	**5.89**	**5.38**

III. RESULTS AND ANALYSIS

A. Performance on Rural Indian Fingerprints

We begin the performance evaluation of the proposed CDC-GAN by assessing its performance on the publicly available Rural Indian fingerprint database [21]. This database has 1631 poor quality fingerprints acquired from the rural Indian population extensively involved in physical labor. As shown in Figure 3, the proposed CDC-GAN improves the fingerprint quality by predicting missing ridge structure due to creases and also improving the contrast between ridges and valleys. Thus, facilitating improved fingerprint quality (Table 1) and matching performance characterized by reduced equal error rate (EER) (Table 2). Corresponding histogram of fingerprint quality scores obtained using NFIQ [22] and detection error trade-off (DET) curves for the Bozorth [22] and the MCC matcher [23]–[25] are presented in Figure 4. These results signify the superior performance of the proposed CDC-GAN compared to state-of-the-art fingerprint denoising algorithms.

B. Performance on Latent Fingerprints

Next, we evaluate the fingerprint denoising performance of the proposed CDC-GAN on the IIITD-MOLF database [26], the largest publicly available database of challenging latent fingerprints with 4400 fingerprint samples. Fingerprints acquired from the Lumidigm fingerprint sensor are used as the samples enrolled in the gallery. As depicted in Figure 5, CDC-GAN outperforms state-of-the-art fingerprint denoising algorithms in predicting ridge information at fingerprint regions with smudged and poor contrast ridge details. Similar trends are reported for fingerprint quality scores (Table 3)

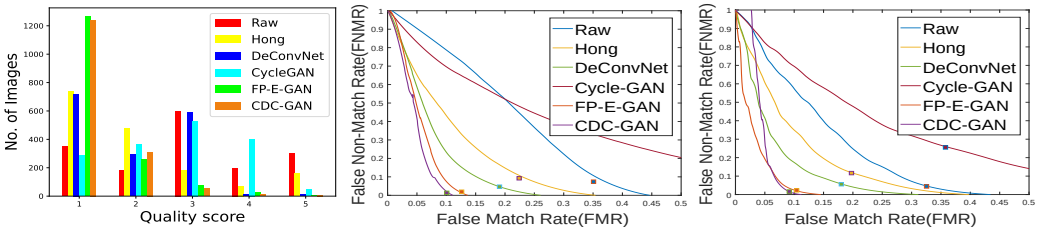

(a) (b) (c)

Fig. 4. (a) Histogram of *Nfiq* fingerprint quality scores and DET curves for (b) Bozorth (c) MCC. Proposed CDC-GAN significantly outperforms state-of-the-art fingerprint denoising algorithms on the rural Indian fingerprint database [21].

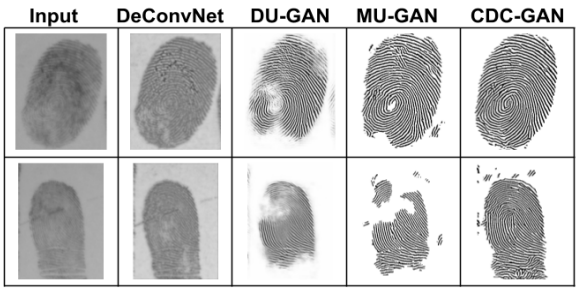

Fig. 5. Sample results obtained on IIITD-MOLF database [26] demonstrating the limitation of state-of-the-art fingerprint denoising methods to recover ridge details in heavily distorted fingerprint regions. On the other hand, the proposed CDC-GAN successfully recovers ridge information in heavily distorted fingerprints regions.

TABLE 3. Average NFIQ fingerprint quality scores obtained on the IIITD-MOLF database [26].

Denoising Algorithm	**NFIQ Score (↓)**
Raw Image	4.96
Cycle-GAN [14]	4.90
DeConvNet [12]	4.09
DU-GAN [17]	3.01
MU-GAN [19]	**1.48**
CDC-GAN	2.38

TABLE 4. Rank-50 accuracy obtained on the IIITD-MOLF database [26].

Denoising Algorithm	**Bozorth (↑)**	**MCC (↑)**
Raw Image	5.45	6.06
Cycle-GAN [14]	6.29	4.65
DeConvNet [12]	14.02	14.27
Svoboda *et al.* [27]	NA	22.36
DU-GAN [17]	23.16	27.21
MU-GAN [19]	25.09	28.61
CDC-GAN	**28.00**	**33.09**

and rank-50 accuracy (Table 4). We note that in poor quality fingerprint regions, DU-GAN does not generate any ridge patterns as opposed to the proposed CDC-GAN, which generates some non-smooth ridge patterns. This explains the unusually better fingerprint quality scores obtained for DU-GAN compared to CDC-GAN. However, since fingerprints generated by DU-GAN have missing ridge information, CDC-GAN significantly outperforms DU-GAN. The corresponding histogram plots of fingerprint quality scores and cumulative matching curve (CMC) are plotted in Figure 6.

C. Ridge Structure Preservation Ability

In order to preserve the identity information, a fingerprint denoising algorithm must be able to preserve ridge information such as orientation and minutiaes. We now head towards quantifying the capability of the proposed CDC-GAN to preserve ridge details while enhancing the ridge structure. Figure 7 (a) presents sample

TABLE 5. Average NFIQ fingerprint quality scores obtained on the Rural Indian fingerprint database during ablation study.

Denoising Algorithm	**NFIQ Score (↓)**
Baseline	1.31
Source	1.32
Target	**1.26**
CDC-GAN	1.30

TABLE 6. Average equal error rate (EER) obtained on the Rural Indian fingerprint database during ablation study.

Denoising Algorithm	**Bozorth (↓)**	**MCC (↓)**
Baseline	7.30	5.96
Source	6.56	5.86
Target	6.10	5.67
CDC-GAN	**5.89**	**5.38**

synthetically distorted and corresponding ground truth binarized fingerprints. A high structural similarity index metric (SSIM) value is obtained between the ground truth and the fingerprints generated by CDC-GAN, which successfully demonstrates the ability of the proposed CDC-GAN to preserve ridge details while enhancing them.

D. Ablation Study

Lastly, we conduct an ablation study to individually quantify the contribution of enforcing cross-domain consistency in source and target domains. We find that enforcing cross-domain consistency clearly helps as its addition renders improved verification performance. In addition, we find that enforcing consistency regularization in the target domain turns out to be more useful than enforcing consistency regularization in the source domain. This is due to the reason that the samples in the target domain are otherwise unseen by the model (if not used to enforce consistency). Subsequently, as anticipated, the best verification performance is achieved after introducing cross-domain consistency loss in both source and target domains. However, fingerprint quality is only marginally improved after introducing cross-domain consistency. Results are reported in Table 5 and Table 6. Samples results are presented in Figure 7 (b).

IV. CONCLUSION AND FUTURE WORK

This paper introduces consistency regularization into the fingerprint denoising domain such that the proposed CDC-GAN is trained to ensure consistency in the output for fingerprints with a similar ridge structure, however varying background, and ridge-valley clarity. Results reveal improved denoising performance obtained by CDC-GAN compared to the state-of-the-art. In the future, we intend to study consistency regularization techniques in the context of different components of an automated fingerprint recognition system, such as presentation attack detection and foreground fingerprint segmentation. Furthermore, in the future, proposed CDC-GAN can be integrated into existing HPC environments [28] and make them more robust.

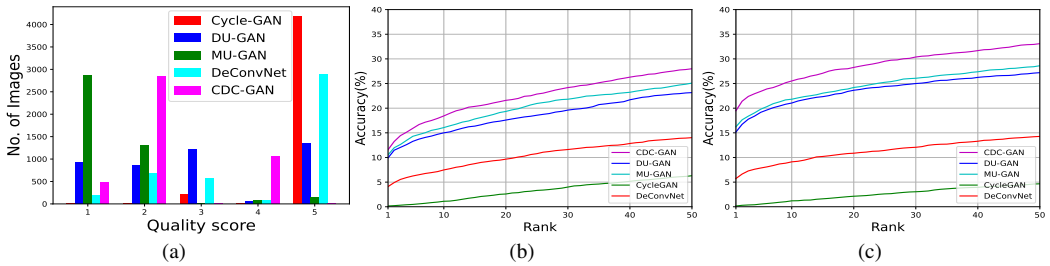

(a) (b) (c)

Fig. 6. (a) Histogram of *Nfiq* fingerprint quality scores and cumulative matching curves (CMC) for (b) Bozorth (c) MCC. Proposed CDC-GAN significantly outperforms state-of-the-art fingerprint denoising algorithms on the IIITD-MOLF database [26].

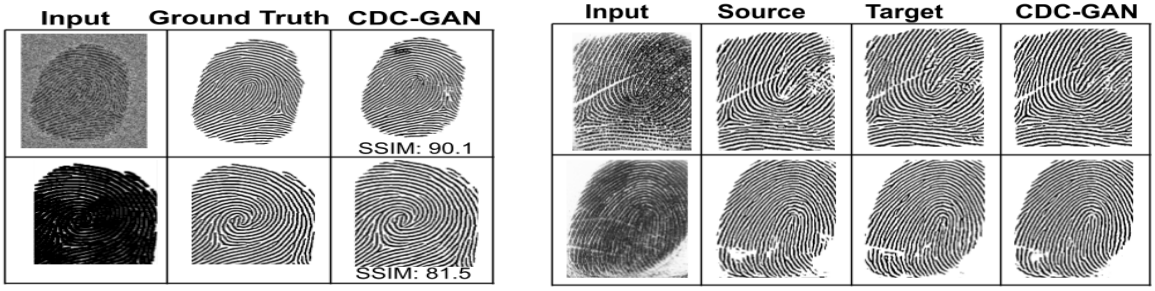

(a) (b)

Fig. 7. Sample cases demonstrating (a) the ridge preservation ability of the proposed CDC-GAN (b) effect of introducing cross-domain consistency in source and target domains.

REFERENCES

[1] V. Anand and V. Kanhangad, "Cross-Sensor Pore Detection in High-Resolution Fingerprint Images," *IEEE Sensors Journal*, vol. 22, no. 1, pp. 555 – 564, 2021.

[2] I. Goel, N. B. Puhan, and B. Mandal, "Deep Convolutional Neural Network for Double-Identity Fingerprint Detection," *IEEE Sensors Letters*, vol. 4, no. 5, pp. 1 – 4, 2020.

[3] V. Anand and V. Kanhangad, "PoreNet: CNN-based Pore Descriptor for High-Resolution Fingerprint Recognition," *IEEE Sensors Journal*, vol. 20, no. 16, pp. 9305 – 9313, 2020.

[4] C. Peng, M. Chen, and X. Jiang, "Under-Display Ultrasonic Fingerprint Recognition with Finger Vessel Imaging," *IEEE Sensors Journal*, vol. 21, no. 6, pp. 7412 – 7419, 2021.

[5] I. Joshi, A. Utkarsh, R. Kothari, V. K. Kurmi, A. Dantcheva, S. Dutta Roy, and P. K. Kalra, "Sensor-Invariant Fingerprint ROI Segmentation using Recurrent Adversarial Learning," in *International Joint Conference on Neural Networks (IJCNN)*, 2021, pp. 1 – 8.

[6] I. Joshi, A. Utkarsh, P. Singh, A. Dantcheva, S. Dutta Roy, and P. K. Kalra, "On Restoration of Degraded Fingerprints," *Multimedia Tools and Applications*, pp. 1–29, 2022.

[7] I. Joshi, "Advanced Deep Learning Techniques for Fingerprint Preprocessing," Ph.D. dissertation, IIT Delhi, 2021.

[8] Y. Li, Q. Xia, C. Lee, S. Kim, and J. Kim, "A Robust and Efficient Fingerprint Image Restoration Method based on a Phase-Field Model," *Pattern Recognition*, vol. 123, p. 108405, 2022.

[9] R. Gupta, M. Khari, D. Gupta, and R. G. Crespo, "Fingerprint Image Enhancement and Reconstruction using the Orientation and Phase Reconstruction," *Information Sciences*, vol. 530, pp. 201 – 218, 2020.

[10] L. Hong, Y. Wan, and A. Jain, "Fingerprint Image Enhancement: Algorithm and Performance Evaluation," *IEEE Transactions on Pattern Analysis and Machine Intelligence*, vol. 20, no. 8, pp. 777 – 789, 1998.

[11] S. Chikkerur, A. N. Cartwright, and V. Govindaraju, "Fingerprint Enhancement using STFT Analysis," *Pattern Recognition*, vol. 40, no. 1, pp. 198 – 211, 2007.

[12] P. Schuch, S. Schulz, and C. Busch, "De-Convolutional Auto-encoder for Enhancement of Fingerprint Samples," in *Proc. International Conference on Image Processing Theory, Tools and Applications (IPTA)*, 2016, pp. 1 – 7.

[13] I. Joshi, A. Anand, S. Dutta Roy, and P. K. Kalra, "On Training Generative Adversarial Network for Enhancement of Latent Fingerprints," in *AI and Deep Learning in Biometric Security*, 2021, pp. 51 – 79.

[14] D. Karabulut, P. Tertychnyi, H. S. Arslan, C. Ozcinar, K. Nasrollahi, J. Valls, J. Vilaseca, T. B. Moeslund, and G. Anbarjafari, "Cycle-Consistent Generative Adversarial Neural Networks based Low Quality Fingerprint Enhancement," *Multimedia Tools and Applications*, vol. 79, no. 25, pp. 18 569 – 18 589, 2020.

[15] I. Joshi, R. Kothari, A. Utkarsh, V. K. Kurmi, A. Dantcheva, S. Dutta Roy, and P. K. Kalra, "Explainable Fingerprint ROI Segmentation using Monte Carlo Dropout," in *IEEE Winter Conference on Applications of Computer Vision Workshops (WACVW)*, 2021, pp. 60 – 69.

[16] I. Joshi, A. Anand, M. Vatsa, R. Singh, S. Dutta Roy, and P. Kalra, "Latent Fingerprint Enhancement using Generative Adversarial Networks," in *IEEE Winter Conference on Applications of Computer Vision (WACV)*, 2019, pp. 895 – 903.

[17] I. Joshi, A. Utkarsh, R. Kothari, V. K. Kurmi, A. Dantcheva, S. Dutta Roy, and P. K. Kalra, "Data Uncertainty Guided Noise-Aware Preprocessing of Fingerprints," in *International Joint Conference on Neural Networks (IJCNN)*, 2021, pp. 1 – 8.

[18] P. Qian, A. Li, and M. Liu, "Latent Fingerprint Enhancement Based on DenseUNet," in *Proc. International Conference on Biometrics (ICB)*, 2019, pp. 1 – 6.

[19] I. Joshi, A. Utkarsh, R. Kothari, V. K. Kurmi, , A. Dantcheva, S. Dutta Roy, and P. K. Kalra, "On Estimating Uncertainty of Fingerprint Enhancement Models," in *Digital Image Enhancement and Reconstruction*, 2022 (accepted).

[20] P. Schuch, S. Schulz, and C. Busch, "Survey on the Impact of Fingerprint Image Enhancement," *IET Biometrics*, pp. 102 – 115, 2017.

[21] C. Puri, K. Narang, A. Tiwari, M. Vatsa, and R. Singh, "On Analysis of Rural and Urban Indian Fingerprint Images," in *Proc. International Conference on Ethics and Policy of Biometrics*, 2010, pp. 55 – 61.

[22] NIST. NBIS- NIST Biometric Image Software. http://biometrics.idealtest.org/.

[23] R. Cappelli, M. Ferrara, and D. Maltoni, "Minutia Cylinder-Code: A New Representation and Matching Technique for Fingerprint Recognition," *IEEE Transactions on Pattern Analysis and Machine Intelligence*, vol. 32, no. 12, pp. 2128 – 2141, 2010.

[24] R. Cappelli, M. Ferrara, and D. Maltoni, "Fingerprint Indexing Based on Minutia Cylinder-Code," *IEEE Transactions on Pattern Analysis and Machine Intelligence*, vol. 33, no. 5, pp. 1051 – 1057, 2010.

[25] M. Ferrara, D. Maltoni, and R. Cappelli, "Noninvertible Minutia Cylinder-Code Representation," *IEEE Transactions on Information Forensics and Security*, vol. 7, no. 6, pp. 1727 – 1737, 2012.

[26] A. Sankaran, M. Vatsa, and R. Singh, "Multisensor Optical and Latent Fingerprint Database," *IEEE Access*, vol. 3, pp. 653 – 665, 2015.

[27] J. Svoboda, F. Monti, and M. M. Bronstein, "Generative Convolutional Networks for Latent Fingerprint Reconstruction," in *Proc. IEEE International Joint Conference on Biometrics (IJCB)*, 2017, pp. 429 – 436.

[28] C. Militello, V. Conti, S. Vitabile, and F. Sorbello, "Embedded Access Points for Trusted Data and Resources Access in HPC Systems," *The Journal of Supercomputing*, vol. 55, no. 1, pp. 4–27, 2011.